

Electronic Supplementary Information (ESI)

**(*E*)-1,2-Diphenylethene-based conjugated nanoporous polymers for
superior adsorptive removal of dye from water**

Ahmed F. Saber^a and Ahmed F. M. EL-Mahdy^{*a}

^aDepartment of Materials and Optoelectronic Science, National Sun Yat-Sen University,
Kaohsiung 80424, Taiwan

*To whom correspondence should be addressed

E-mail: ahmedelmahdy@mail.nsysu.edu.tw

Section	Content	Page No.
S1	Characterization	S3
S2	Synthetic Procedures of monomers	S4
S3	Synthetic Procedures of CMPs	S7
S4	FTIR and NMR Spectral Profiles of Monomers	S8
S5	FTIR Spectral Profiles of CMPs	S11
S6	Thermal gravimetric analysis of CMPs	S13
S7	Powder X-ray diffraction of CMPs	S14
S8	X-ray photoelectron spectroscopy of CMPs	S14
S9	Powder X-ray diffraction of CMPs after dye removal	S15
S10	Organic Pollutant Treatment in Water	S16
S11	References	S18

S1. Characterization

Fourier-transform infrared spectroscopy (FTIR). FTIR spectra were recorded using a Bruker Tensor 27 FTIR spectrophotometer and the conventional KBr plate method; 32 scans were collected at a resolution of 4 cm^{-1} .

Solid state nuclear magnetic resonance (SSNMR) spectroscopy. SSNMR spectra were recorded using a Bruker Avance 400 NMR spectrometer and a Bruker magic-angle-spinning (MAS) probe, running 32,000 scans.

Thermogravimetric analysis (TGA). TGA was performed using a TA Q-50 analyzer under a flow of N_2 . The samples were sealed in a Pt cell and heated from 40 to 800 $^{\circ}\text{C}$ at a heating rate of 20 $^{\circ}\text{C min}^{-1}$ under N_2 at a flow rate of 50 mL min^{-1} .

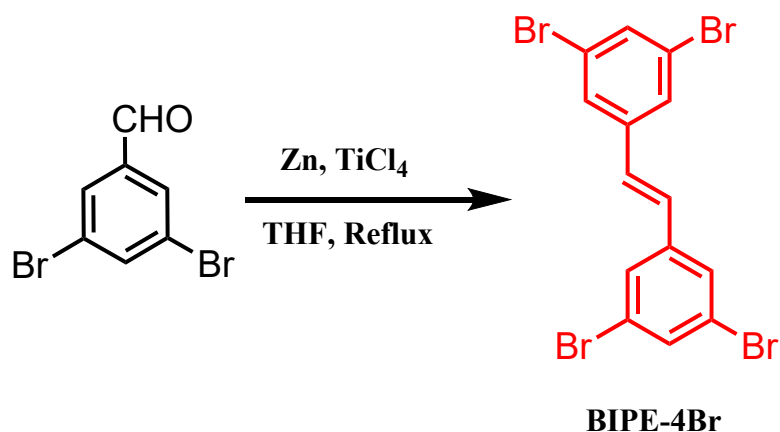
Surface area and porosimetry (ASAP/BET). The BET surface areas and porosimetry investigations of the prepared samples (ca. 20–100 mg) were conducted using a Micromeritics ASAP 2020 Surface Area and Porosity analyzer. Nitrogen isotherms were generated through incremental exposure to ultrahigh-purity N_2 (up to ca. 1 atm) in a liquid N_2 (77 K) bath.

Field-emission scanning electron microscopy (FE-SEM). FE-SEM was performed using a JEOL JSM-7610F scanning electron microscope. Samples were subjected to Pt sputtering for 100 s prior to observation.

Transmission electron microscopy (TEM). TEM was accomplished using a JEOL-2100 scanning electron microscope, operated at 200 kV.

UV–Vis–NIR spectroscopy. UV–Vis–NIR spectra were recorded at 25 $^{\circ}\text{C}$ using a Jasco V-570 spectrometer, with deionized water as the solvent. Raman spectra were recorded at 25 $^{\circ}\text{C}$ using a Jobin–Yvon T6400 micro Raman apparatus, with a He–Cd laser (325 nm line) as an excitation source.

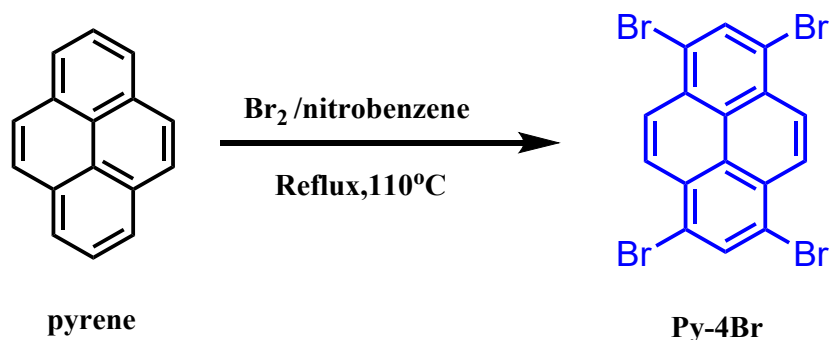
S2. Synthetic Procedures of Monomers



Scheme S1. Synthesis of 1,3,6,8-tetrabromopyrene (BIPE-4Br).

Synthesis of (*E*)-1,2-bis(3,5-dibromophenyl)ethene (BIPE-4Br) [S1,S2]

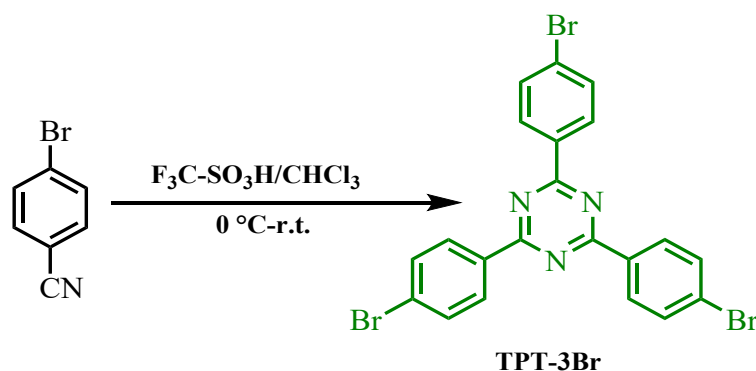
In a dry 250 mL three-necked flask both of zinc metal (4.2 g, 64.2 mmol, 5.6 eq) and THF were charged (150 mL). The resulting suspension was allowed to cool to 0°C in an ice bath/acetone for 10 min. before the gradual addition of TiCl₄ (5.4 g, 3.2 mL, 28.2 mmol, 2.3 eq). Then, a calculated amount (3.0 g, 11.4 mmol, 1 eq) of 3,5-dibromobenzaldehyde was added and the mixture heated to reflux. 24 hrs. later, the reaction was cooled to ambient temperature (25°C) and tempered dropwise with water (20 mL). All solvents were eliminated by rotary evaporation, and extraction of the obtained solid was carried out using chloroform (3 x 250 mL). The extracted liquor was further concentrated by rotary evaporation, to give the desired solid which was sonicated with acetone (25 mL) and filtered, yielding (2.68 g, 5.41 mmol, 57 %) as a white crystalline solid. ¹H-NMR (300 MHz, CDCl₃, δ): δ 7.58 (m, 2H, ph.), 7.55 (m, 4H, ph.), 6.93 (s, 2H, 2CH ethene); ¹³C-NMR (75 MHz, CDCl₃, δ): δ 140.03, 133.63, 128.62, 128.51, 123.51. MS (HR-EI), m/z calcd. C₁₄H₈Br₄ [M]⁺ 495.7319, found 495.7318.



Scheme S2. Synthesis of 1,3,6,8-tetrabromopyrene (Py-4Br).

Synthesis of 1,3,6,8-Tetrabromopyrene (Py-4Br) [S3].

Bromine's solution (2.3 mL, 44 mmol) in nitrobenzene (20 mL) was added to pyrene's solution (2.00 g, 10 mmol) in nitrobenzene (20 mL). Then the obtained mixture was heated under reflux for a period of 4 h at 120 °C till appearance of a green precipitate. This solid was washed with ethanol, filtered off, and dried under vacuum at 50 °C to give the desired Py-Br₄ (4.4 g, 89%). FTIR (KBr, cm⁻¹): 3053 (aromatic C-H stretching), 682 (C-Br stretching).

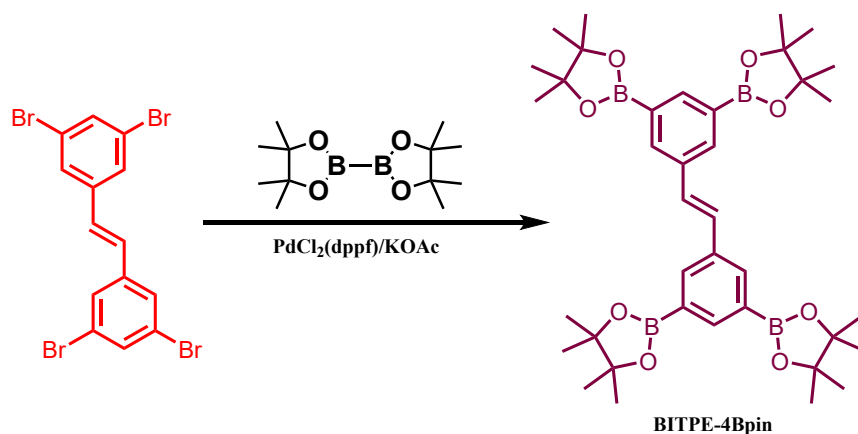


Scheme S3. Synthesis of 2,4,6-tris(4-bromophenyl)-1,3,5-triazine (TPT-3Br).

Synthesis of 2,4,6-tris(4-bromophenyl)-1,3,5-triazine (TPT-3Br) [S4,S5]

A solution of 4-bromobenzonitrile (1.5 g, 8.24 mmol) in dry chloroform (20 mL) under nitrogen atmosphere was cooled to 0 °C and then trifluoromethanesulfonic acid (4 mL, 0.045 mmol) was added gradually in small portions. The previous solution was stirred for 0.5 h. at 0 °C before warming to room temperature. Stirring was continued for an additional 20 h at room temperature, subsequently, the reaction mixture was poured into ice-water (50 mL), and

neutralization using sodium carbonate (Na_2CO_3) was carried out. The solid gained was gathered by filtration and dried overnight under vacuum to produce a white solid of TPT- Br_3 . FT-IR (powder): 1578, 1518, 1400, 1372, 1173, 1069, 1011, 843, 806, 498 cm^{-1} . $^1\text{H-NMR}$ (500 MHz, CDCl_3 , δ): 8.60 (d, $J = 8.5$ Hz, 6H), 7.70 (d, $J = 8.5$ Hz, 6H). $^{13}\text{C-NMR}$ (125 MHz, CDCl_3 , δ): 171.22, 134.91, 132.01, 130.48, 127.88.

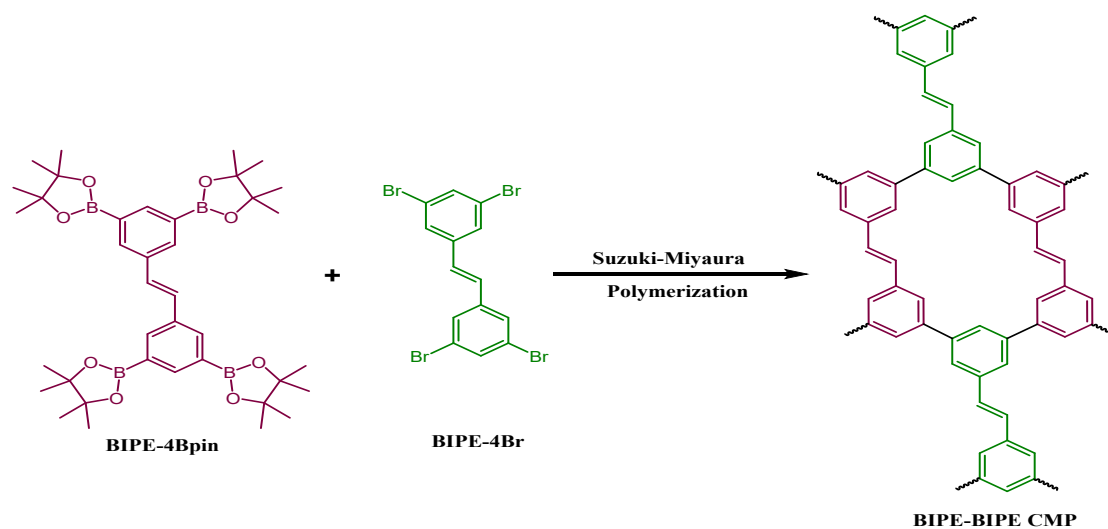


Scheme S4. Synthesis of (*E*)-1,2-bis(3,5-bis(4,4,5,5-tetramethyl-1,3,2-dioxaborolan-2-yl)phenyl)ethene (BITPE-4Bpin)

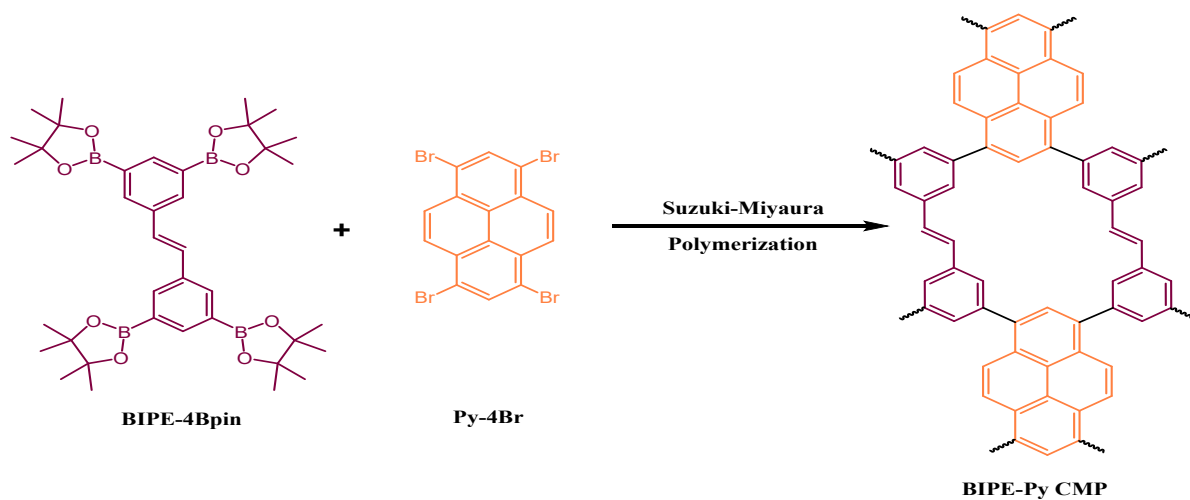
Synthesis of (*E*)-1,2-bis(3,5-bis(4,4,5,5-tetramethyl-1,3,2-dioxaborolan-2-yl)phenyl)ethene (BITPE-4Bpin)

In a dried and cleaned 100 mL two neck-bottle, a mix of (*E*)-1,2-bis(3,5-dibromophenyl)ethene (BIPE-4Br) (1.0 g, 5.8 mmol), bis(pinacolato)-diboron (3.06 g, 34.7 mmol), potassium acetate (1.217 g, 35.7 mmol), and 1,1'-Bis(diphenylphosphino)ferrocene]dichloropalladium (II) (0.127 g, 0.50 mmol) in *p*-dioxane (50 mL) was heated at 100 °C under nitrogen atmosphere for 2 days. Then, the reaction mixture was allowed to cool to room temperature, to be poured into iced-water. The formed precipitate was collected by extraction with dichloromethane and dried under vacuum overnight. The residue was purified by flash chromatographically (SiO_2 ; THF/Hexane = 1:4) to provide a white solid (0.56 g, 75.0%). FTIR (KBr, cm^{-1}): 3112, 2980, 1596, 1324. $^1\text{H-NMR}$ (CDCl_3 , 25 °C, 500 MHz): 8.06-8.15 (m, 6H), 7.24 (d, 2H), 1.36 (s, 48H). $^{13}\text{C-NMR}$ (CDCl_3 , 25 °C, 125 MHz): 140.20, 135.75, 128.41, 83.52, 24.31.

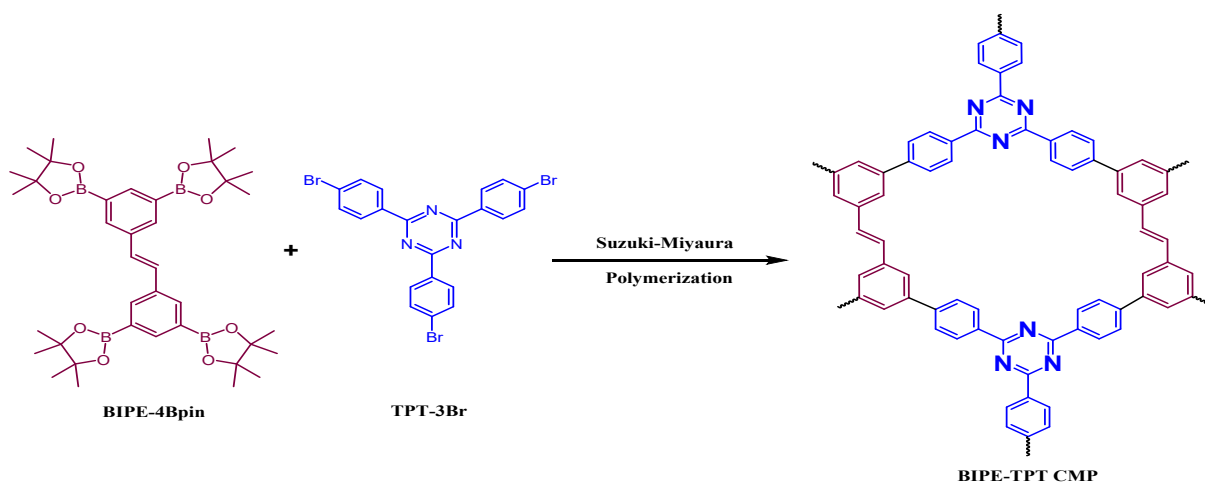
S3. Synthetic Procedures of CMPs



Scheme S5. Synthesis of BIPE-BIPE-CMP.



Scheme S6. Synthesis of BIPE-Py-CMP.



Scheme S7. Synthesis of BIPE-TPT CMP.

S4. FTIR and NMR Spectral Profiles of Monomers

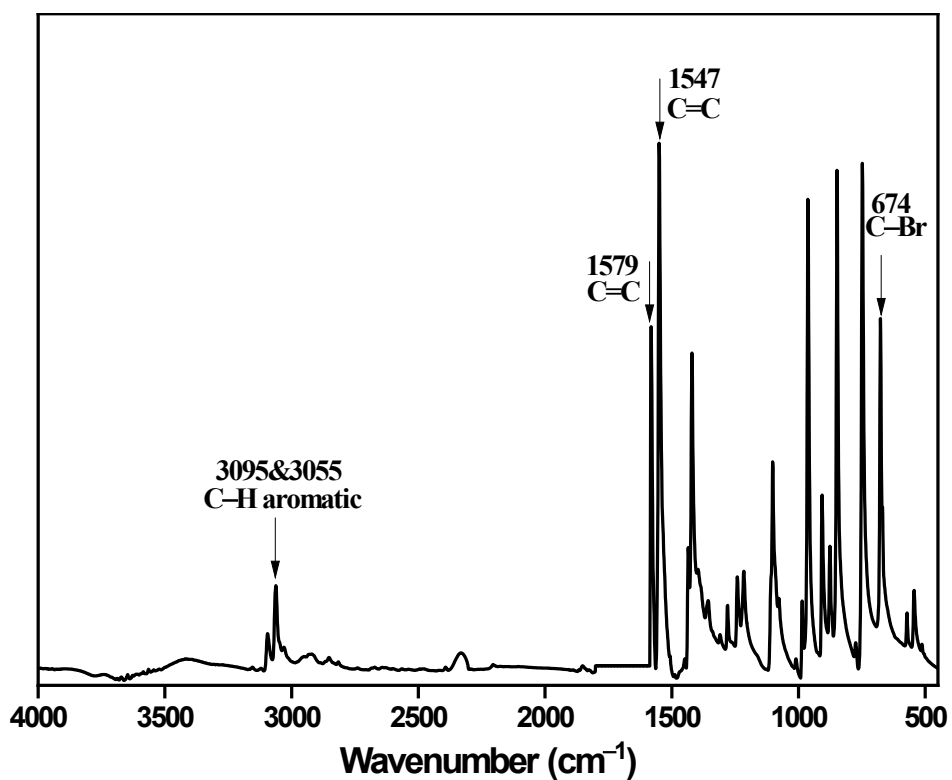


Fig. S1 FTIR spectrum of (*E*)-1,2-bis(3,5-dibromophenyl)ethene (BIPE-4Br).

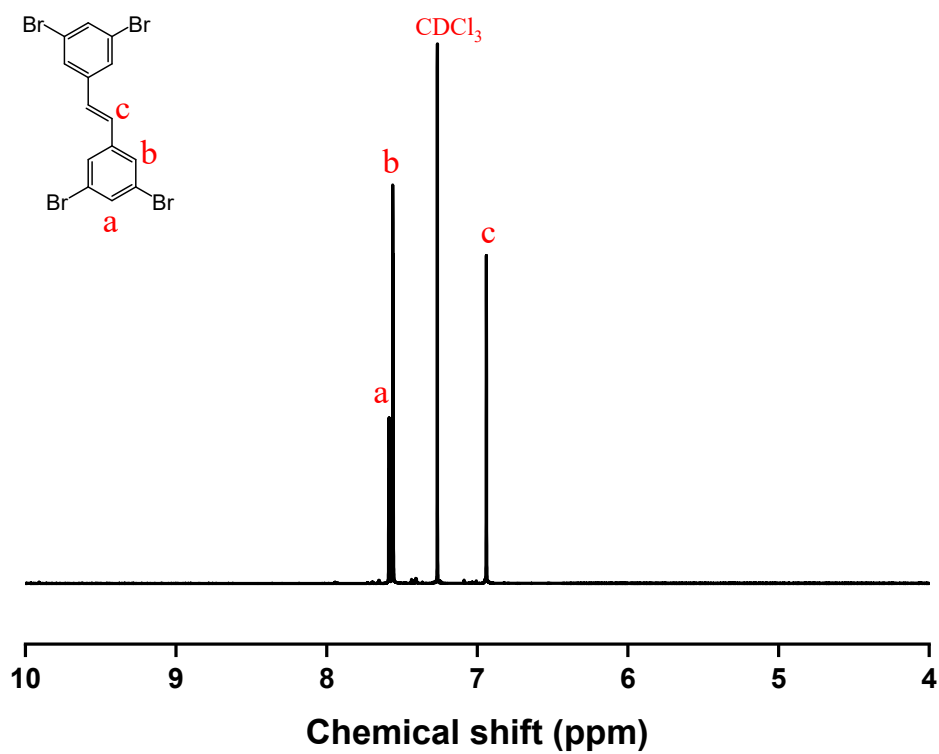


Fig. S2 ¹H NMR spectrum of (*E*)-1,2-bis(3,5-dibromophenyl)ethane (BIPETH-4Br).

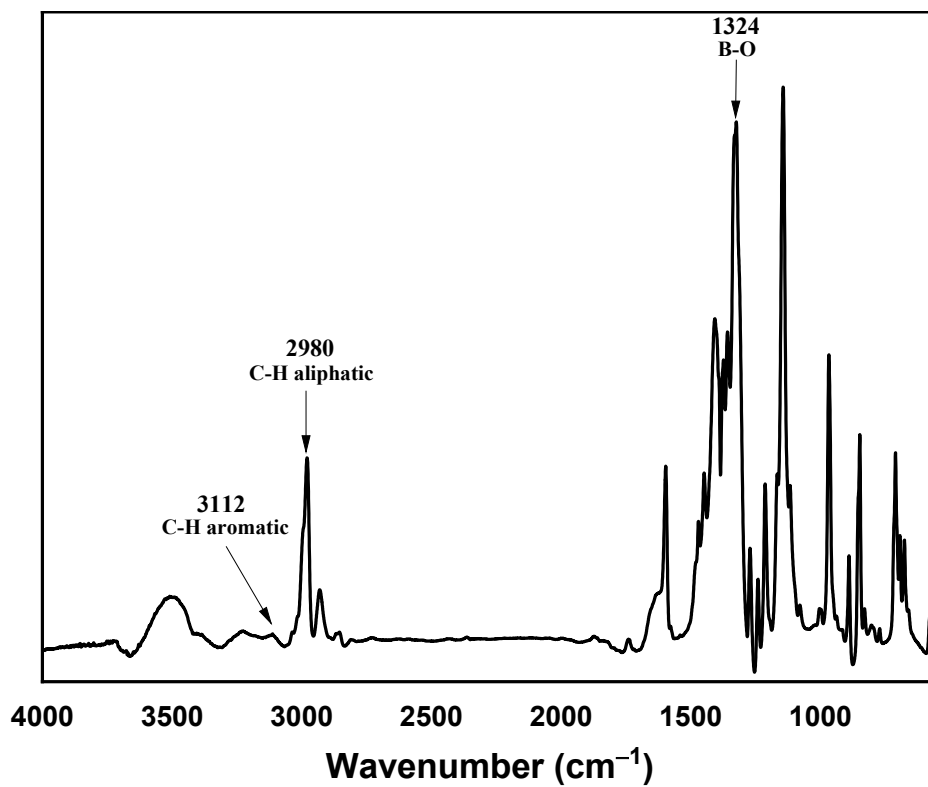


Fig. S3 FTIR spectrum of (*E*)-1,2-bis(3,5-bis(4,4,5,5-tetramethyl-1,3,2-dioxaborolan-2-yl)phenyl)-ethene (BITPE-4Bpin).

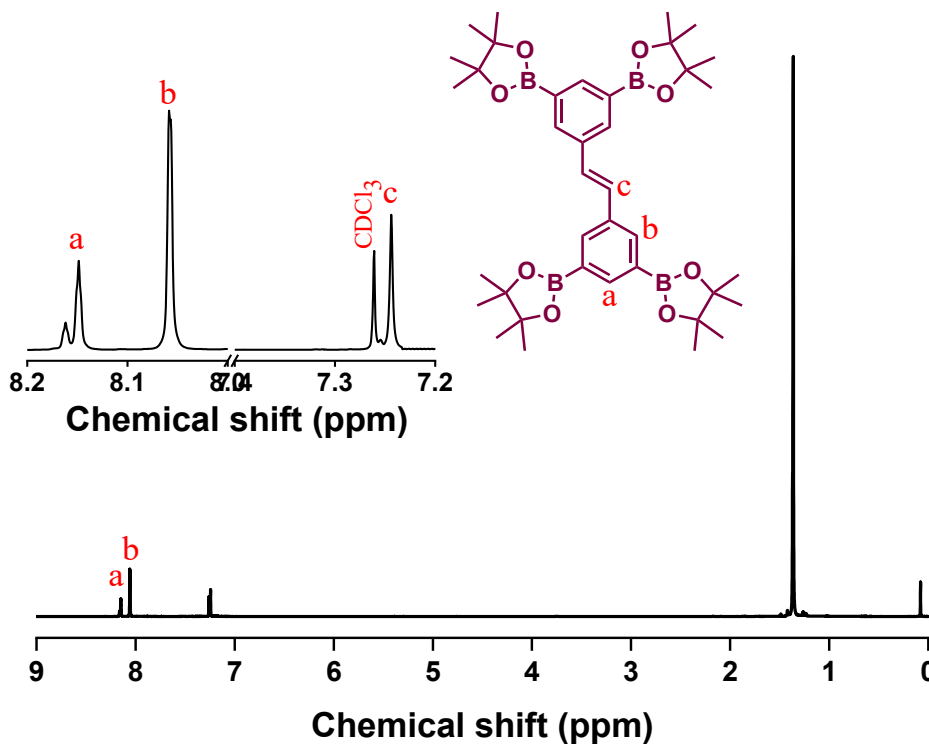


Fig. S4 ¹H NMR spectrum of (*E*)-1,2-bis(3,5-bis(4,4,5,5-tetramethyl-1,3,2-dioxaborolan-2-yl)phenyl)-ethene (BITPE-4Bpin).

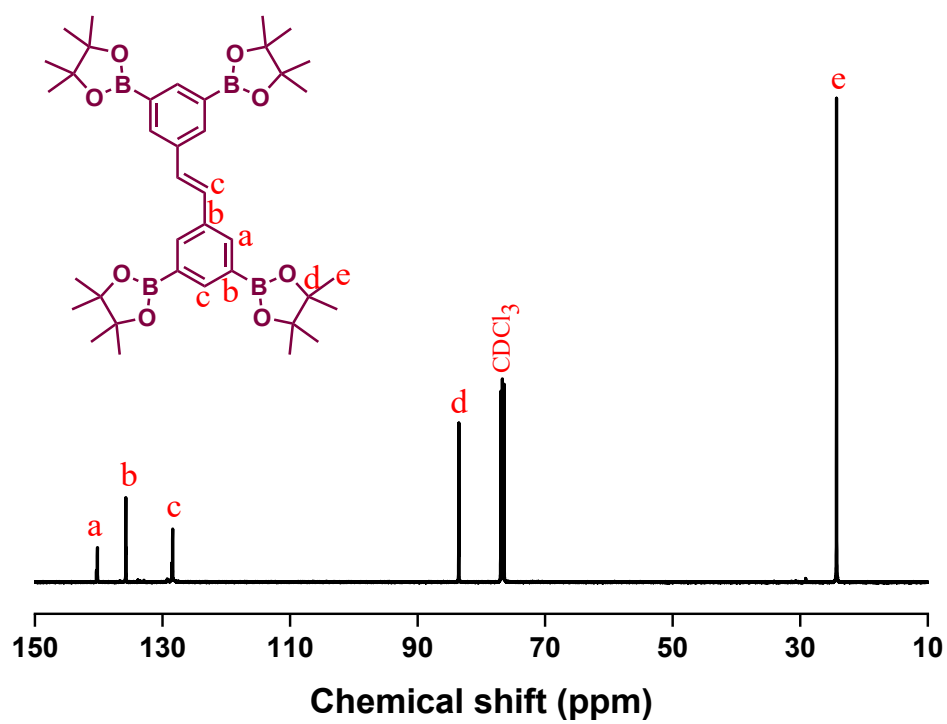


Fig. S5 ¹³C NMR spectrum of (*E*)-1,2-bis(3,5-bis(4,4,5,5-tetramethyl-1,3,2-dioxaborolan-2-yl)phenyl)-ethene (BITPE-4Bpin).

S5. FTIR Spectral Profiles of CMPs

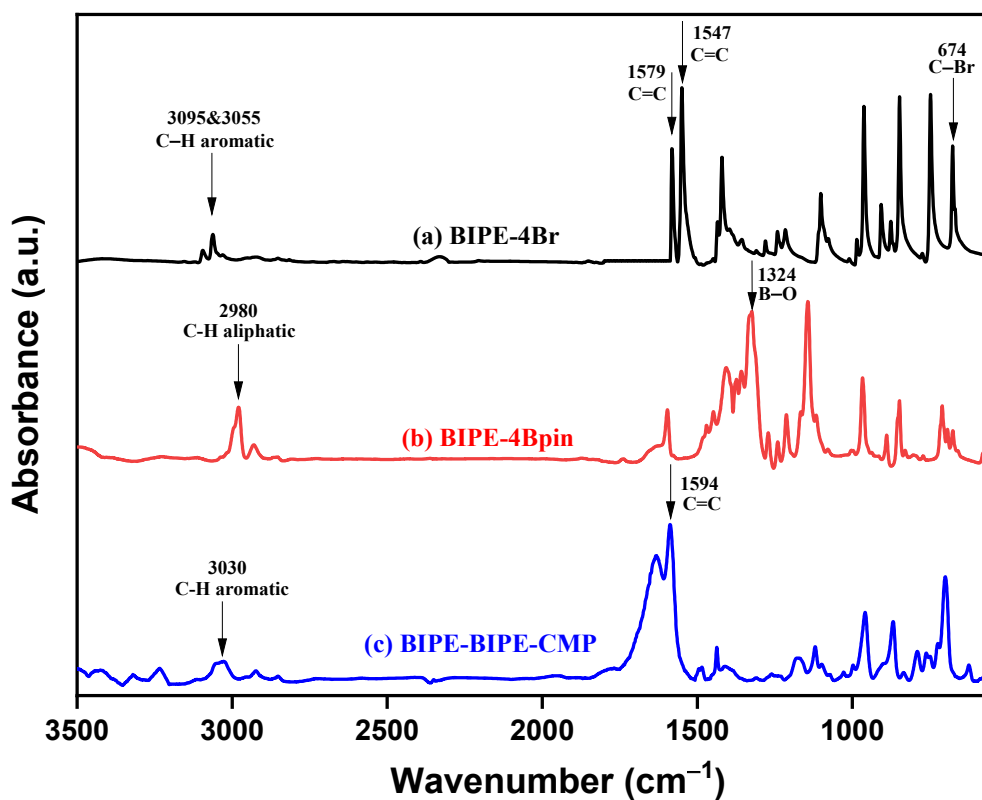


Fig. S6 FTIR spectra of (a) BIPE-4Br, (b) BIPE-4Bpin, and (c) BIPE-BIPE-CMP.

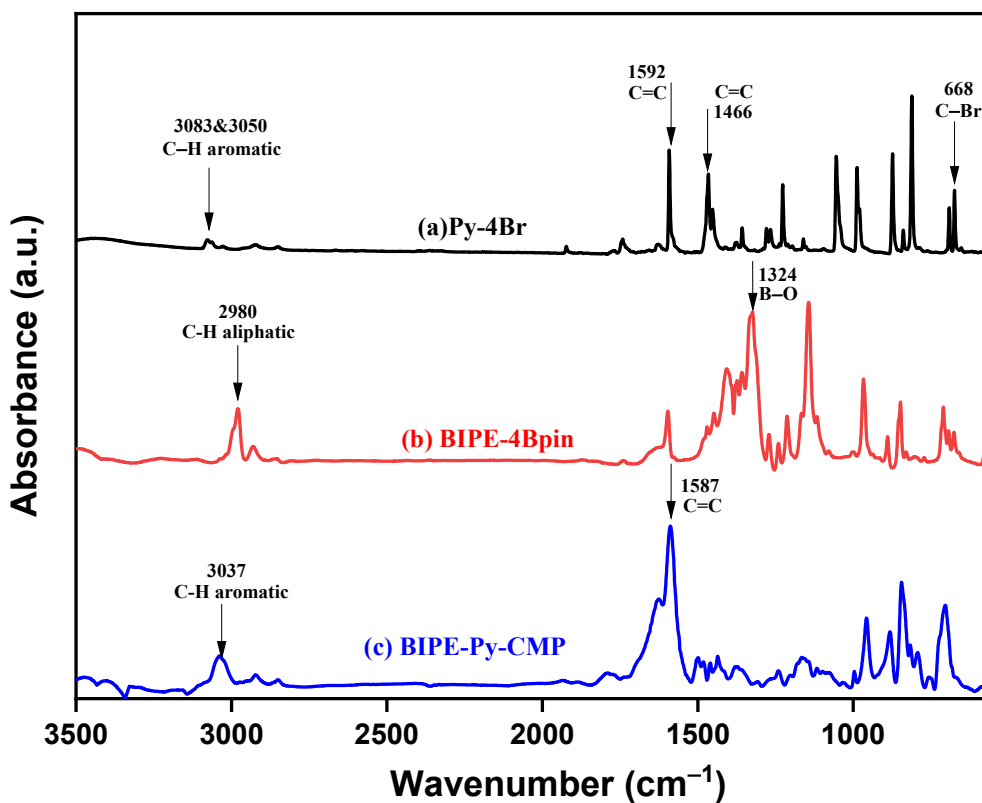


Fig. S7 FTIR spectra of (a) Py-4Br, (b) BIPE-4Bpin, and (c) BIPE-Py-CMP.

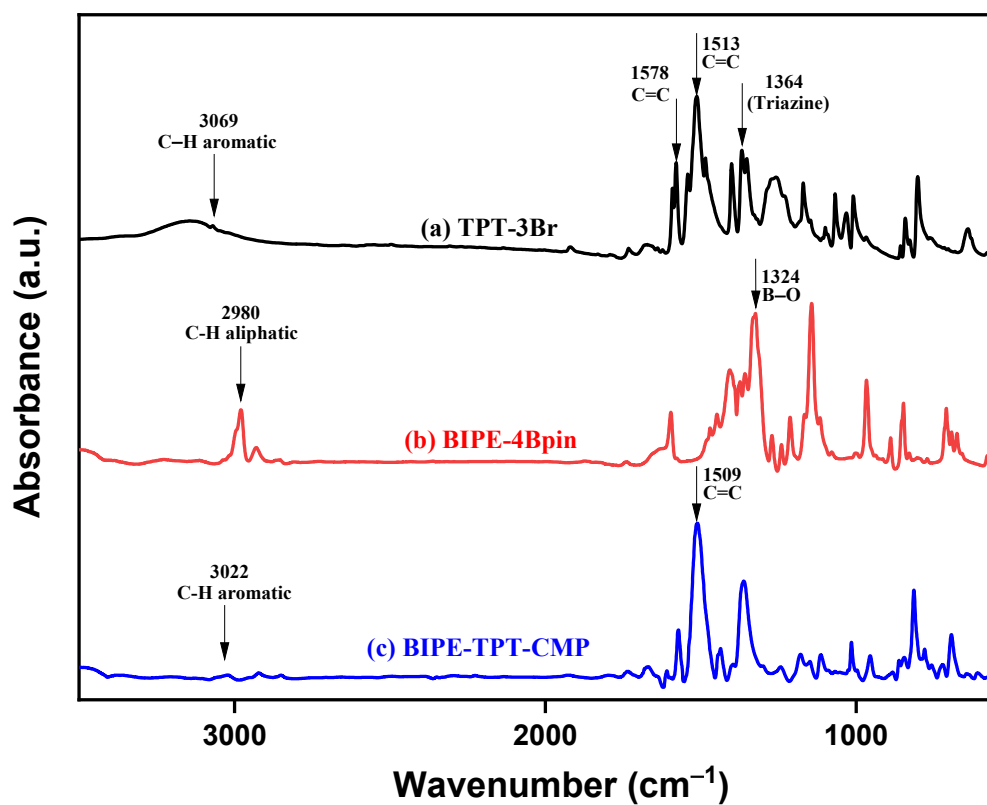


Fig. S8 FTIR spectra of (a) TPT-3Br, (b) BIPE-4Bpin, and (c) BIPE-TPT-CMP.

S6. Thermal gravimetric analysis of CMPs

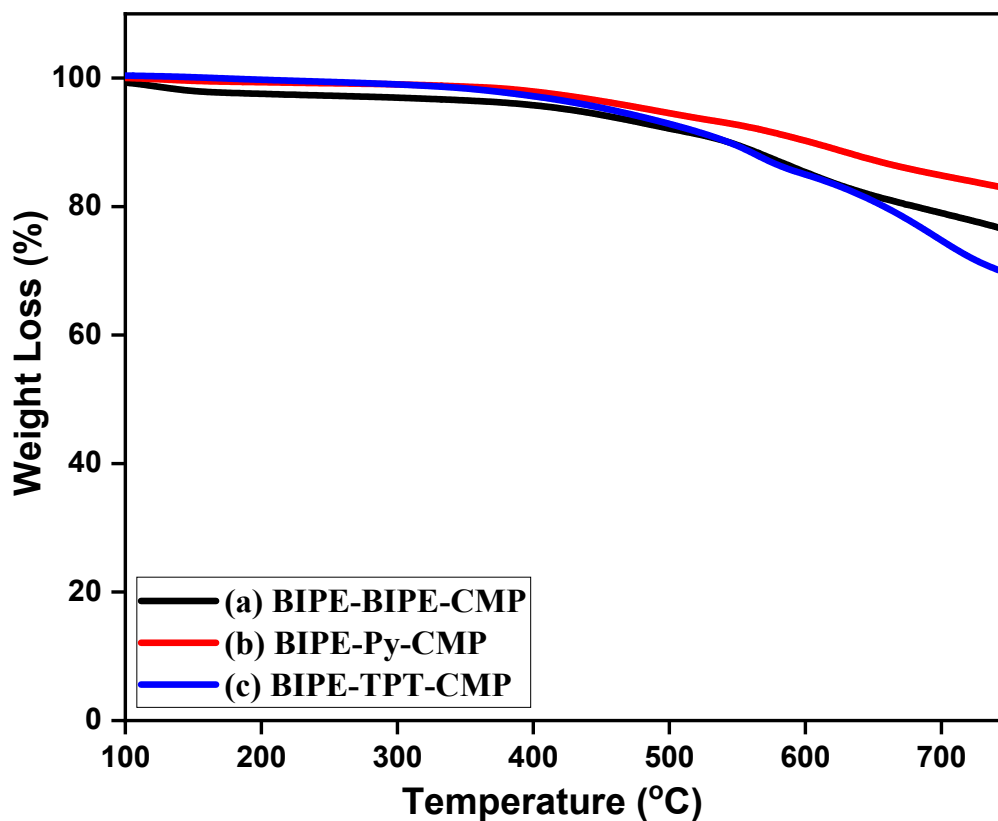


Fig. S9 TGA curves of (a) BIPE-BIPE-CMP, (b) BIPE-Py-CMP, and (c) BIPE-TPT-CMP.

Table S1. Values of $T_{d10\%}$ and Char yield of CMPs.

	$T_{d5\%}$ (°C)	$T_{d10\%}$ (°C)	Char yield (%)
BIPE-BIPE-CMP	429	543	74
BIPE-Py-CMP	488	604	81
BIPE-TPT-CMP	457	543	67

S7. Powder X-ray diffraction of CMPs

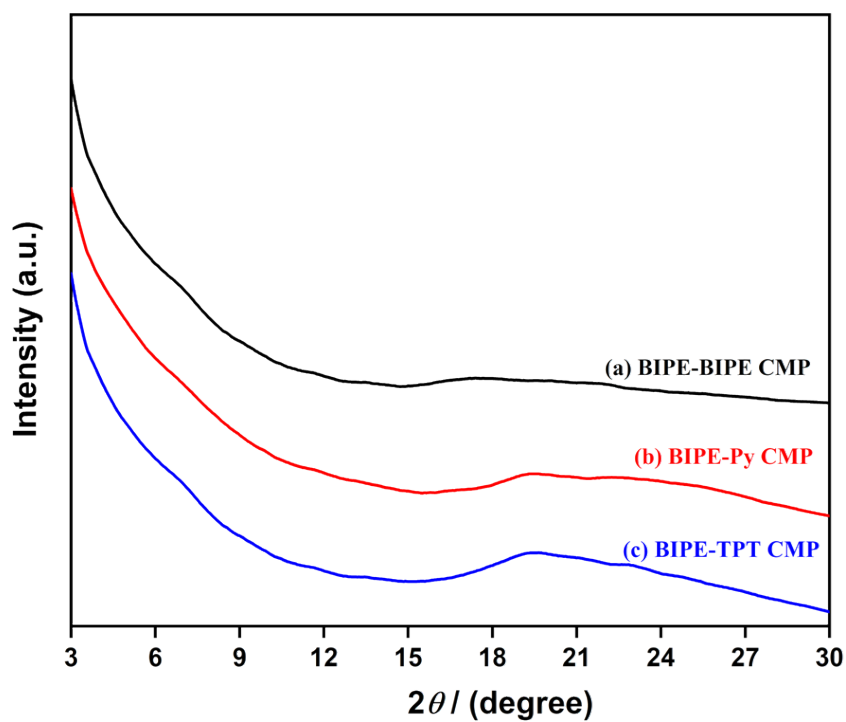


Fig. S10 powder X-ray diffraction patterns of (a) BIPE-BIPE-CMP, (b) BIPE-Py-CMP, and (c) BIPE-TPT-CMP.

S8. X-ray photoelectron spectroscopy of CMPs

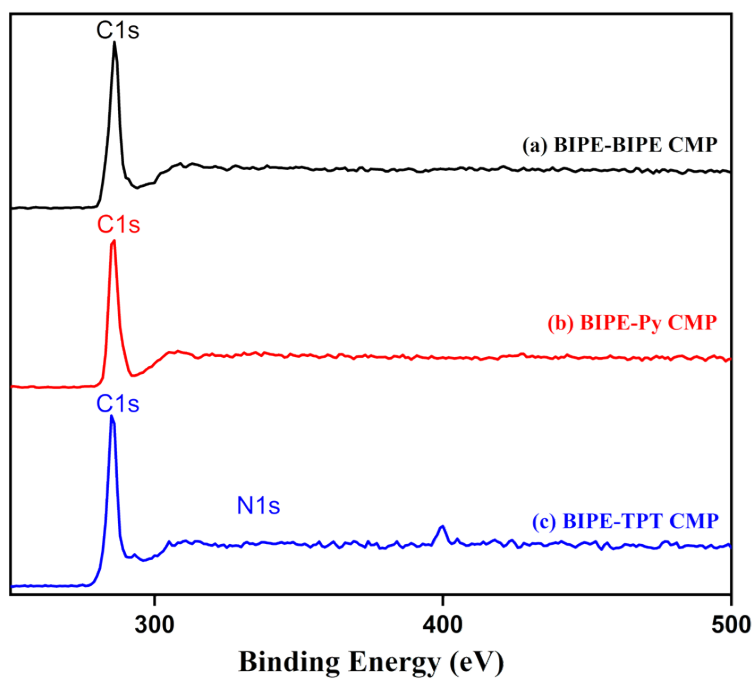


Fig. S11 XPS spectra of (a) BIPE-BIPE-CMP, (b) BIPE-Py-CMP, and (c) BIPE-TPT-CMP.

S9. Powder X-ray diffraction of CMPs after dye removal

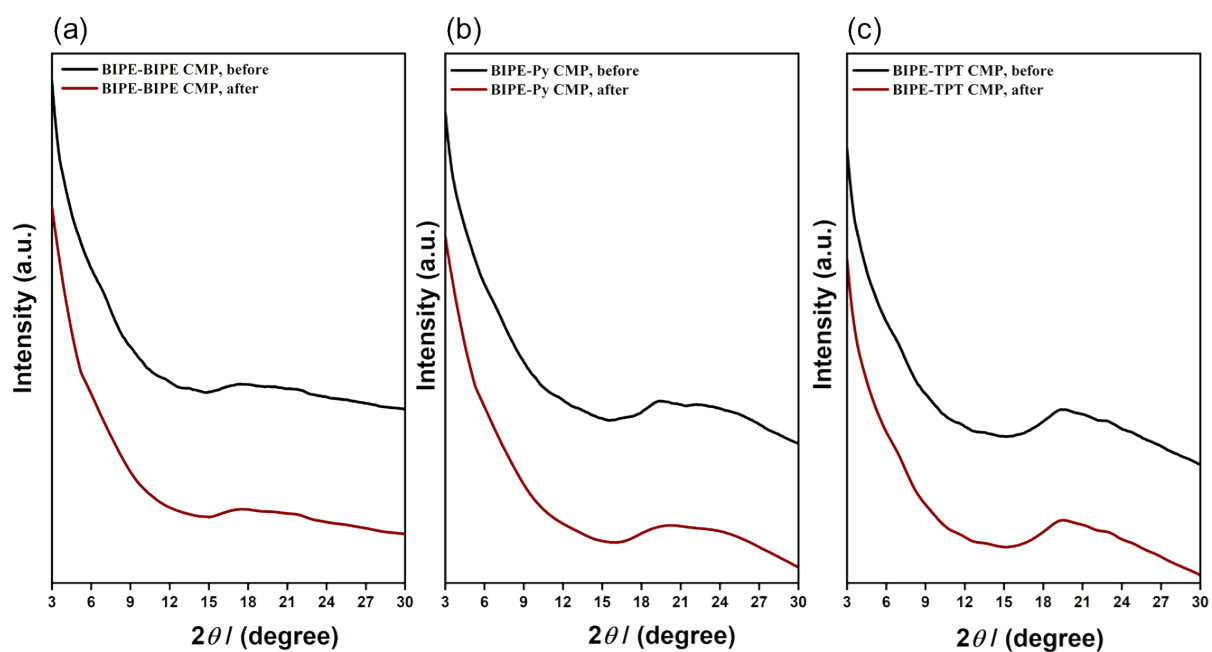


Fig. S12 powder X-ray diffraction patterns of (a) BIPE-BIPE-CMP, (b) BIPE-Py-CMP, and (c) BIPE-TPT-CMP before and after the sixth regeneration cycle.

S10. Organic Pollutant Treatment in Water

Table S2. Maximum adsorption capacities of RhB on the BIPE-BIPE, BIPE-Py, and BIPE-TPT CMPs, compared with those of other reported materials.

Adsorbent	Dye	Q_m (mg g ⁻¹)	BET(m ² g ⁻¹)	Amount/dye conc.	Temperature	pH	Ref.
Graphene sponge	RhB	72	150	2 mg ml ⁻¹ /95 mg l ⁻¹	298	S6
Nanoporous PDVB-VI-0.2	RhB	260	737	0.5 mg ml ⁻¹ /50 mg l ⁻¹	298-318	3-11	S7
S1	RhB	200	48.6	0.08 mg ml ⁻¹ /40 mg l ⁻¹	298	S8
activated carbon (OAC)	RhB	312-409	543	0.1-1.5 mg ml ⁻¹ /100-450 mg l ⁻¹	298-318	1.63-10.31	S9
Mesoporous carbon (ST-A)	RhB	83-100	670	0.03-0.7 mg ml ⁻¹ /30-310 mg l ⁻¹	298-315	S10
N-doped mesoporous gyroid carbon	RhB	204	491	0.5 mg ml ⁻¹ /12.5-150 mg l ⁻¹	298	S11
CMP-YA	RhB	535	1410	0.2 mg ml ⁻¹ /25 mg l ⁻¹	298	S12
Py-BF-CMP	RhB	1905	1306	0.2 mg ml ⁻¹ /25 mg l ⁻¹	298	S13
TPE-BF-CMP	RhB	1024	777	0.2 mg ml ⁻¹ /25 mg l ⁻¹	298	S13
TPA-BF-CMP	RhB	926	590	0.2 mg ml ⁻¹ /25 mg l ⁻¹	298	S13
Ttba-TPDA-COF	RhB	833	726	0.5 mg ml ⁻¹ /20-800 mg l ⁻¹	298	2-11	S14
CuP-DMNDA-COF/Fe	RhB	378-429	273	0.25 mg ml ⁻¹ /16 mg l ⁻¹	293-313	S15
BIPE-BIPE	RhB	352	918	0.4 mg ml ⁻¹ /25 mg l ⁻¹	298	This work
BIPE-Py	RhB	1027	1400	0.4 mg ml ⁻¹ /25 mg l ⁻¹	298	This work
BIPE-TPT	RhB	739	903	0.4 mg ml ⁻¹ /25 mg l ⁻¹	298	This work

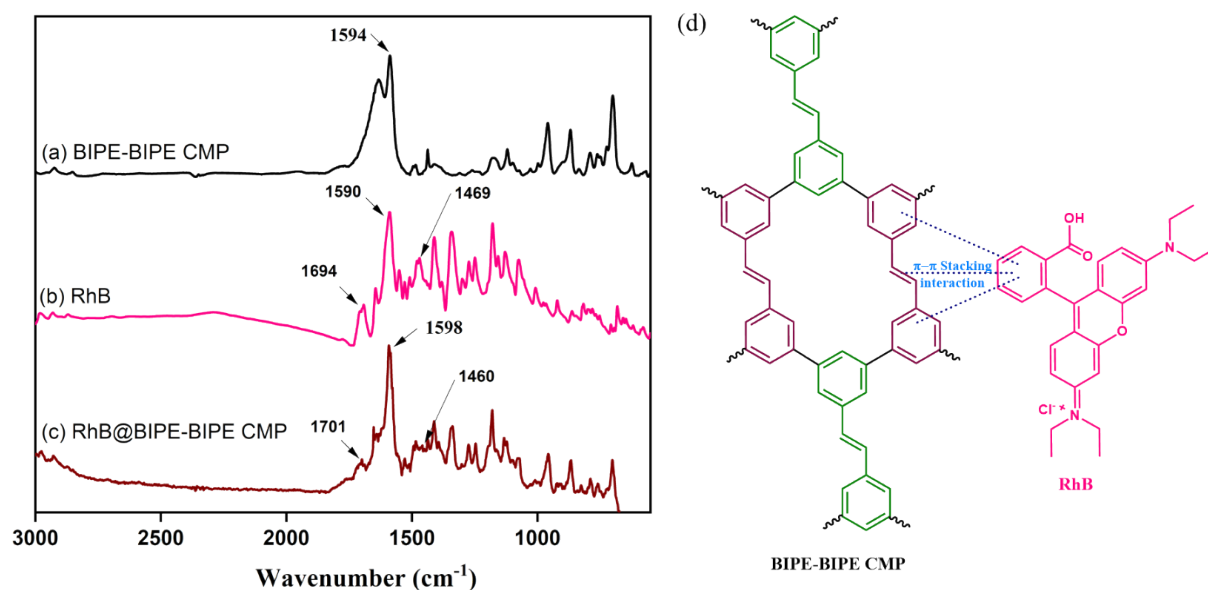


Fig. S13 FT-IR spectra of (a) BIPE-BIPE CMP, (b) rhodamine B (RhB), and (c) BIPE-BIPE CMP after adsorbed rhodamine B. (d) Adsorption mechanism of rhodamine B on BIPE-BIPE CMP.

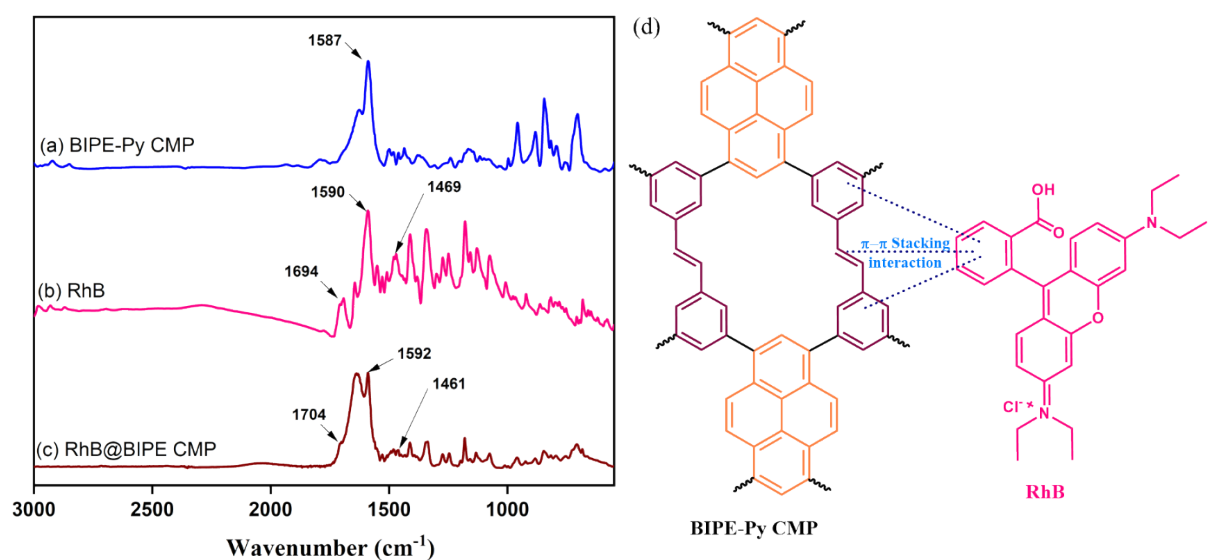


Fig. S14 FT-IR spectra of (a) BIPE-Py CMP, (b) rhodamine B (RhB), and (c) BIPE-Py CMP after adsorbed rhodamine B. (d) Adsorption mechanism of rhodamine B on BIPE-Py CMP.

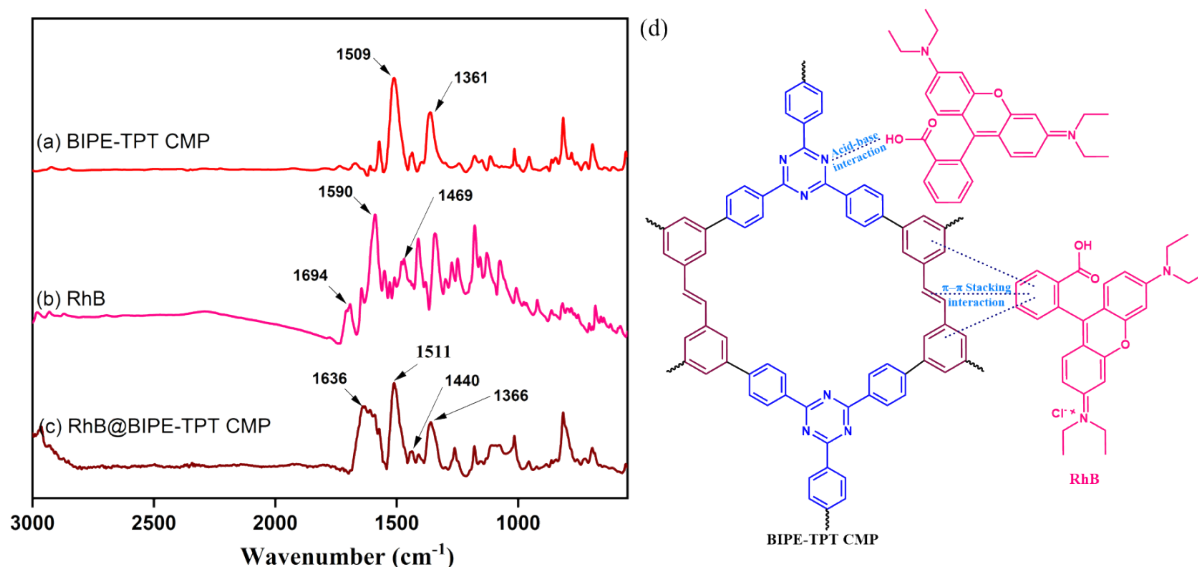


Fig. S15 FT-IR spectra of (a) BIPE-TPT CMP, (b) rhodamine B (RhB), and (c) BIPE-TPT CMP after adsorbed rhodamine B. (d) Adsorption mechanism of rhodamine B on BIPE-TPT CMP.

S11. References

- [S1] B. Das, K. Vankateswarlu, A. Majhi, V. Siddaiah and K. R. Reddy, *J. Mol. Catal.*, 2007, **267**, 30-33.
- [S2] A. Raman, G. Augustine, N. Ayyadurai and S. Easwaramoorthi, *J. Mater. Chem. C*, 2018, **6**, 10497-10501.
- [S3] M. G. Mohamed, M. H. Elsayed, A. M. Elewa, A. F. EL-Mahdy, C.-H. Yang, A. A. K. Mohammed, H-H. Chou and S.-W. Kuo, *Catal. Sci. Technol.*, 2021, **11**, 2229-2241.
- [S4] A. F. M. EL-Mahdy, C. H. Kuo, A. Alshehri, C. Young, Y. Yamauchi, J. Kim and S. W. Kuo, *J. Mater. Chem. A*, 2018, **6**, 19532-19541.
- [S5] A. F. M. EL-Mahdy, C. Young, J. Kim, J. You, Y. Yamauchi and S. W. Kuo, *ACS Appl. Mater. Interfaces*, 2019, **11**, 9343-9354.
- [S6] J. Zhao, W. Ren and H. M. Cheng, *J. Mater. Chem.*, 2012, **22**, 20197-20202.
- [S7] Y. Han, W. Li, J. Zhang, H. Meng, Y. Xu and X. Zhang, *RSC Adv.*, 2015, **5**, 104915-104922.
- [S8] S. Wang, B. Yang and Y. Liu, *J. Colloid Interface Sci.*, 2017, **507**, 225-233.
- [S9] O. Üner, Ü. Geçgel, H. Kolancılar and Y. Bayrak, *Chem. Eng. Commun.*, 2017, **204**, 772-783.
- [S10] K. Jedynak, D. Wideł and N. Redzia, *Colloids Interfaces*, 2019, **3**, 30.
- [S11] A. F. M. EL-Mahdy, T. E. Liu and S. W. Kuo, *J. Hazard. Mater.*, 2020, **391**, 122163.
- [S12] Y. Yuan, H. Huang, L. Chen and Y. Chen, *Macromolecules*, 2017, **50**, 4993-5003.
- [S13] B. Wang, Z. Xie, Y. Li, Z. Yang and L. Chen, *Macromolecules*, 2018, **51**, 3443-3449.
- [S14] T. Xu, S. An, C. Peng, J. Hu and H. Liu, *Ind. Eng. Chem. Res.*, 2020, **59**, 8315-8322.
- [S15] Y. Hou, X. Zhang, C. Wang, D. Qi, Y. Gu, Z. Wang and J. Jiang, *New J. Chem.*, 2017, **41**, 6145-6151.